3D QSAR Studies of Mps1 (TTK) Kinase Inhibitors Based on CoMFA

Pavithra K. Balasubramanian[1†], Anand Balupuri[1†], and Seung Joo Cho[1,2†]

Abstract

Monopolar spindle 1 (Mps1) is an attractive cancer target due to its high expression levels in a wide range of cancer cells. Mps1 is a dual specificity kinase. It plays an essential role in mitosis. The high expression od Mps1 was observed in various grades of breast cancers. In the current study, we have developed a CoMFA model of pyridazine derivatives as Mps1 kinase inhibitors. The developed CoMFA model (q^2=0.797; ONC=6; r^2=0.992) exhibited a good predictive ability. The model was then validated by Leave out five, progressive sampling and bootstrapping and found to be robust. The analysis of the CoMFA contour maps depicted favorable and unfavorable regions to enhance the activity. Bulky positive substitution at R^3 position and Negative substitution in R^1 position is favored could increase the activity. In contrast, bulky substitution in R^1 position is not favored. Our results can be used in designing a potent Mps1 (TTK) inhibitor.

Keywords: CoMFA, Monopolar Spindle Kinase (Mps1), TTK Kinase, Pyridazine Derivatives, Kinase Inhibitors

1. Introduction

Protein kinases are critical regulators of cell division. The mitotic kinases include Polo, Aurora, Bub, NEK/NimA, and MPS1 kinases[1]. The monopolar spindle (MPS1) gene was first identified in the yeast, Saccharomyces cerevisiase[2]. Mps1 also called as TTK kinase. Mps1 is a dual specificity kinase that can phosphorylate serines/threonines and tyrosines. Mps1 function as the key kinase that activates the spindle assembly checkpoint (SAC)[3]. Along with other cellular processes, MPS1 kinases also function in multiple roles in mitosis, including spindle pole duplication[4], mitotic checkpoint signaling, mitotic cytokinesis and the maintenance of CIN[5,6]. Mps1 also found be involved in the genotoxic stress response such as DNA damage[7].

Mps1 expression is found in proliferating cells during mitosis. Overexpression of Mps1 is observed in a various cancer cell lines and and tumor types, including anaplastic thyroid carcinoma, breast cancer, and lung cancers[8-11]. Based on the role Mps1 plays in mitosis and cell division, it is considered as one of the most promising drug targets for cancer therapy[12]. Several compounds that have

Mps1 inhibitory activity have been identified and their anticancer activity has been studied[13,14]. BAY1161909 and BAY1217389 are the two highly selective Mps1 inhibitor that are in phase 1 clicnical trials[3]. Our research group has reported several review and research articles on insilico techniques such molecular docking and 3D-QSAR studies[15-19]. In this study, we have performed a ligand-based CoMFA study on series of pyridylpyrazolopyridine derivatives have carried out.

2. Methodology

2.1. CoMFA Model

A series of 25 pyridazine derivatives reported by Kusakabe et al., was taken for the study[14]. The logarithmic values of the activities were used. The co-crystallized structure of compound **21** of this series was used as a template to sketch the rest of the molecules in the dataset. All the structures of the dataset were drawn using sketch program of SybylX2.1[20]. The geometry of the molecules was optimized using sybyl Tripos force field and Gasteiger charges were applied. The molecules taken for the study are shown in Table 1. The energy cut off of 30.0 kcal/mol was used and CoMFA model[21] was developed for the dataset molecules. A leave-one-out (LOO) PLS was performed to determine the cross-validated r^2 (q^2) and the optimum number of components and minimum standard error of prediction (SEP) in the model.

Departments of [1]Bio-New Drug Development and [2]Cellular·Molecular Medicine, College of Medicine, Chosun University, Gwangju 501-759, Republic of Korea

†Corresponding author : pavithrabioinfo@gmail.com, anandbalupuri.niper@gmail.com, chosj@chosun.ac.kr

Table 1. Structure and Biological values of pyridazine derivatives as Mps1 kinase inhibitors

Compound	R^1	R^2	R^3	X	Y	pIC_{50}
1	isopropyl (CH_3, CH_3)	cyclopropyl	-	-	-	7.260
2	isopropyl (CH_3, CH_3)	cyclobutyl	-	-	-	6.745
3	isopropyl (CH_3, CH_3)	isopropyl (CH_3, CH_3)	-	-	-	6.337
4	isopropyl (CH_3, CH_3)	H	-	-	-	5.602
5	i-Bu	cyclopropyl	-	-	-	7.161
6	n-Pr	cyclopropyl	-	-	-	6.310
7	i-Pr	cyclopropyl	-	-	-	6.886
8	cyclopropylmethyl	cyclopropyl	-	-	-	7.409
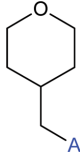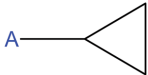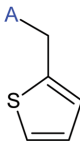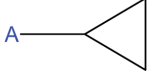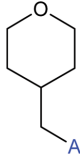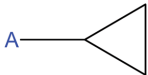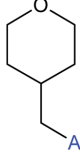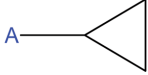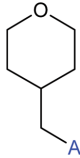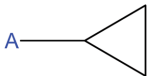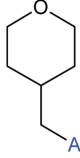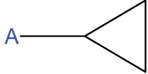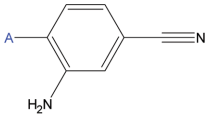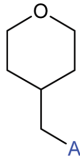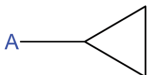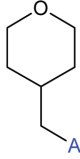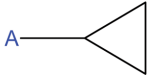
Table 1. Continued

9			-	-	-	7.456
10			-	-	-	7.237
11			Ph	CH	N	8.071
12			P-(CN)Ph	CH	N	8.181
13			P-(CN)Ph	N	CH	8.377
14				N	CH	8.602
15			cyclohexyl	-	-	8.125
16			Ph	-	-	8.168

Table 1. Continued

No.	Structure		Group			Value
17			*p*-(F)Ph	-	-	8.252
18			*o*-(F)Ph	-	-	8.181
19			*o*-(OH)Ph	-	-	8.585
20			Ph	-	-	7.886
21			cyclohexyl	-	-	8.181
22			cyclohexyl	-	-	8.276
23			*i*-Pr	-	-	8.260
24			*t*-Bu	-	-	8.208
25				-	-	8.553

2.2. CoMFA Validation

The developed model was validated to check its predictability using Leave-out-five, bootstrapping and progressive sampling. Bootstrapping of 100 runs and progressive sampling of 100 samplings with 2 to 100 bins was used to validate the models.

3. Results and Discussion

3.1. CoMFA Model

CoMFA model was developed for a series of pyridazine derivatives All the molecules were aligned over the template (compound 10) using alignment method based on the common substructure. The alignment of the dataset is shown in Fig. 2. A reliable CoMFA model

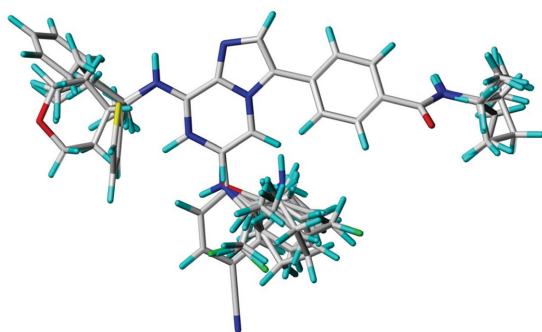for the complete set of dataset compounds was developed (q^2=0.797, NOC=6, r^2=0.992) using Gasteiger charges as partial charge. The model exhibited excellent statistical values in terms of q^2 and r^2 values. The total number of compounds in the dataset is less than 30, hence the data set was not divided into training set and test set. The model was validated using Leave-out-five, bootstrapping and progressive sampling methods. The Leave-out-five value for the model was found to be 0.815. The progressive sampling (Q2) of 100 runs gave the value of 0.648. The bootstrapping r^2 mean (BS-r^2) and BS- standard deviation (BS-SD) was 0.996 and 0.002 respectively. The overall quality of the model was found to be predictable and robust. The detailed tabulation of the developed model is shown in Table 2. The experimental and predicted activity values of the mol-

Fig. 1. Alignment of all the dataset molecules

Table 2. Statistical summary of the developed CoMFA model

Parameters	CoMFA MODEL
q^2	0.797
NOC	6
SEP	0.423
r^2	0.992
SEE	0.082
F value	388.471
LOF	0.812
BS r^2	0.996
BS SD	0.02
Q^2	0.648

q^2: cross-validated correlation coefficient; NOC: Number of components; SEP: Standard Error of prediction; r^2: non-validated correlation coefficient; SEE: Standard Error of Estimation; F value: F-test value; LOF: Leave-out-Five; BS-r^2: Bootstrapping r^2 mean; BS-SD: Bootstrapping Standard deviation; Q^2: progressive sampling.
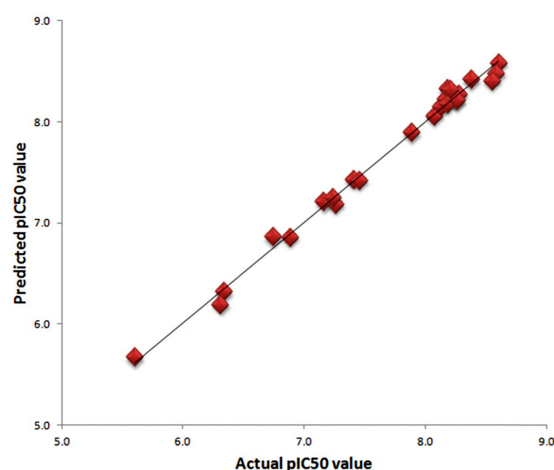

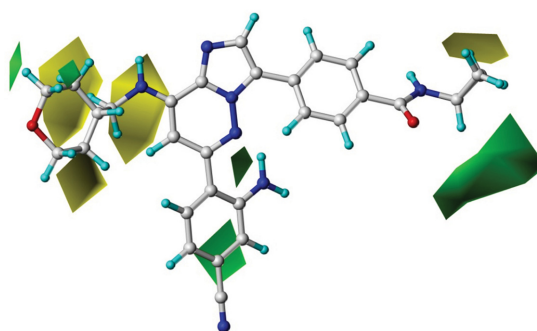**Fig. 2.** Scatter plot diagram of the CoMFA model

Fig. 3. CoMFA Steric contour map. The green contours show sterically favored regions and the yellow contours show the sterically unfavorable regions.

Table 3. Actual versus predicted pIC$_{50}$ with their residuals values of the developed CoMFA model

Compound	Actual pIC$_{50}$	CoMFA	
		Predicted	Residual
1	7.260	7.185	0.075
2	6.745	6.861	-0.116
3	6.337	6.316	0.021
4	5.602	5.668	-0.066
5	7.161	7.207	-0.046
6	6.310	6.192	0.118
7	6.886	6.858	0.028
8	7.409	7.425	-0.016
9	7.456	7.416	0.040
10	7.237	7.250	-0.014
11	8.071	8.056	0.014
12	8.181	8.221	-0.040
13	8.377	8.416	-0.040
14	8.602	8.579	0.023
15	8.125	8.144	-0.019
16	8.168	8.219	-0.051
17	8.252	8.214	0.038
18	8.181	8.326	-0.146
19	8.585	8.479	0.106
20	7.886	7.891	-0.005
21	8.181	8.175	0.006
22	8.276	8.272	0.004
23	8.260	8.211	0.048
24	8.208	8.320	-0.113
25	8.553	8.402	0.151

ecules obtained for the CoMFA model is tabulated in Table 3. The scatter plot and contour map for the same are shown in Fig. 2 and Fig. 3 respectively.

3.2. CoMFA Contour Analysis

The contour maps for the CoMFA model were developed by using standard Coefficient field type with default 80% and 20% level contributions for favorable and unfavorable regions in order. Compound 14, the most active molecule in the dataset is shown superimposed inside the contour map. The steric contour map of the ligand-based CoMFA is shown in Fig. 3a. The favorable region is shown in green color contour; the unfavorable regions are shown in yellow color contours. A big green colour contour near the R^2 position indicates that bulky substitution in that region could increase the activity of the compound. Bulky substitu-
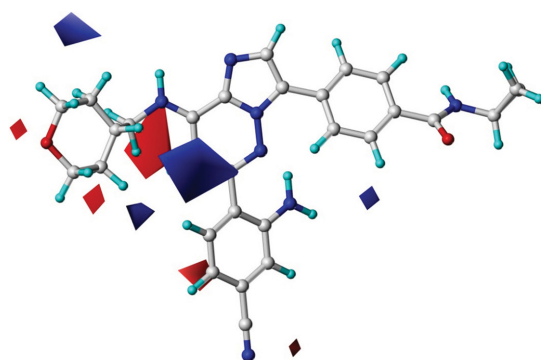
Fig. 4. CoMFA Electrostatic contour map. The blue color regions favor positive substituents and red color region favors negative substitutions.

tion in this region could interact with active site residues Lys553 and Ile663. This interaction was observed with the co-crystallized compound 21 of the dataset molecule[15]. Similarly green contour near the R^3 position suggest that bulky substitution is favored in this position. This can be seen with increase in activity of compounds 13, 17, 19, 22 and 25 including the most active compound 14 that contain bulky substitution in this position. The yellow contours near the R^1 position suggest that bulky substitution at this position is not favored.

The electrostatic contour map of the CoMFA model is shown in Fig. 4. Blue color indicates that positive charge is favored and red color indicates that negative charge is favored to increase the activity of the compound. The small blue contour seen near the R^3 substitution signifies that presence of positive substitution could increase the activity. This is because, the positive substation in that region could find into the hydrophobic pocket of the active site and can interact with residue Met671 and Pro673. This validates the high activity of compounds 17, 22, 23 and 25 including the most active compound 14 that contains positive substitution at this position. The red contour near the NH of R^1 position indicates that negative substitution in that position could increase the activity. Negative substitution at this position could interact with hinge region residues Gly605 and Asn606.

4. Conclusions

Due to the high expression of the Mps1 kinase in var-

ious breast cancers, it becomes an attractive drug target. In the current study, we have taken a series of pyridazine derivatives as potent Mps (TTK) kinase inhibitor. A reasonable CoMFA model was developed with good predictive values. The developed model was subjected to validation tests such as Leave-out-Five, bootstrapping and progressive sampling. The model exhibited excellent predictability. Moreover, the contour maps analysis of the CoMFA model showed the favorable and unfavorable regions to increase the activity of the compounds. The overall contour map analysis implies that bulky substitution at R^2 and R^3 position could increase the activity whereas; bulky substitution in R1 position is not favored. Positive substation in R3 position and Negative substation in R1 position is favored to increase the activity of the compounds. The useful information obtained in our study could be useful to design a more potent inhibitor of pyridazine series.

Acknowledgements

References

[1] X. Liu and M. Winey, "The MPS1 family of protein kinases", Annu. Rev. Biochem., Vol. 81, pp. 561-585, 2012.

[2] M. Winey, L. Goetsch, P. Baum, and B. Byers, "MPS1 and MPS2: novel yeast genes defining distinct steps of spindle pole body duplication", The Journal of Cell Biology, Vol.114, pp. 745-754, 1991.

[3] A. M. Wengner, G. Siemeister, M. Koppitz, V. Schulze, D. Kosemund, U. Klar, D. Stoeckigt, R. Neuhaus, P. Lienau, B. Bader, S. Prechtl, M. Raschke, A.-L. Frisk, O. von Ahsen, M. Michels, B. Kreft, F. von Nussbaum, M. Brands, D. Mumberg, and K. Ziegelbauer, "Novel Mps1 kinase inhibitors with potent antitumor activity", Mol. Cancer Ther., Vol. 15, pp. 583-592, 2016.

[4] A. R. Schutz and M. Winey, "New alleles of the yeast MPS1 gene reveal multiple requirements in spindle pole body duplication", Mol. Biol. Cell, Vol. 9, pp. 759-774, 1998.

[5] A. Abrieu, L. Magnaghi-Jaulin, J. A. Kahana, M. Peter, A. Castro, S. Vigneron, T. Lorca, D. W. Cleveland, and J.-C. Labbé, "Mps1 is a kineto-chore-associated kinase essential for the vertebrate mitoticCheckpoint", Cell, Vol. 106, pp. 83-93, 2001.

[6] V. M. Stucke, H. H. W. Silljé, L. Arnaud, and E. A. Nigg, "Human Mps1 kinase is required for the spindle assembly checkpoint but not for centrosome duplication", EMBO J., Vol. 21, pp. 1723-1732, 2002.

[7] H. A. Fisk, C. P Mattison, and M. Winey, "Human Mps1 protein kinase is required for centrosome duplication and normal mitotic progression", P. Natl. Acad. Sci, U.S.A., Vol. 100, pp. 14875-14880, 2003.

[8] K. Nihira, N. Taira, Y. Miki, and K. Yoshida, "TTK/ Mps1 controls nuclear targeting of c-Abl by 14-3-3-coupled phosphorylation in response to oxidative stress", Oncogene, Vol. 27, pp. 7285-7295, 2008.

[9] J. Daniel, J. Coulter, J. H. Woo, K. Wilsbach, and E. Gabrielson, "High levels of the Mps1 checkpoint protein are protective of aneuploidy in breast cancer cells", P. Natl. Acad. Sci. U.S.A., Vol. 108, 5384-5389, 2011.

[10] M. T. Landi, T. Dracheva, M. Rotunno, J. D. Figueroa, H. Liu, A. Dasgupta, F. E. Mann, J. Fukuoka, M. Hames, A. W. Bergen, S. E. Murphy, P. Yang, A. C. Pesatori, D. Consonni, P. A. Bertazzi, S. Wacholder, J. H. Shih, N. E. Caporaso, and J. Jen, "Gene expression signature of cigarette smoking and its role in lung adenocarcinoma development and survival", Plos One, Vol. 3, pp. e1651, 2008.

[11] G. Salvatore, T. C. Nappi, P. Salerno, Y. Jiang, C. Garbi, C. Ugolini, P. Miccoli, F. Basolo, M. D. Castellone, A. M. Cirafici, R. M. Melillo, A. Fusco, M. L. Bittner, and M. Santoro, "A cell proliferation and chromosomal instability signature in anaplastic thyroid Carcinoma", Cancer Res., Vol. 67, pp. 10148-10158, 2007.

[12] B. Yuan, Y. Xu, J.-H. Woo, Y. Wang, Y. K. Bae, D.-S. Yoon, R. P. Wersto, E. Tully, K. Wilsbach, and E. Gabrielson, "Increased expression of mitotic checkpoint genes in breast cancer cells with chromosomal instability", Clin. Cancer Res., Vol. 12, pp. 405-410, 2006.

[13] E Manchado, M Guillamot, and M. Malumbres, "Killing cells by targeting mitosis", Cell Death Differ., Vol. 19, pp. 369-377, 2012.

[14] K.-I. Kusakabe et al., "Discovery of imidazo[1,2-b]pyridazine derivatives: selective and orally available Mps1 (TTK) kinase inhibitors exhibiting remarkable antiproliferative activity", J. Med. Chem., Vol. 58, 1760-1775, 2015.

[15] P. K. Balasubramanian, A. Balupuri, and S. J. Cho, "A CoMFA study of phenoxypyridine-based JNK3 inhibitors using various partial charge schemes", J. Chosun Natural Sci., Vol. 7, pp. 45-49, 2014.

[16] P. K. Balasubramanian and S. J. Cho, "HQSAR analysis on novel series of 1-(4-phenylpiperazin-1-yl-2-(1H-pyrazol-1-yl) ethanone derivatives targeting CCR1", J. Chosun Natural Sci., Vol. 6, pp. 163-169, 2013.

[17] A. Balupuri and S. J.Cho, "Exploration of the binding mode of indole derivatives as potent HIV-1 inhibitors using molecular docking simulations", J. Chosun Natural Sci., Vol. 6, pp. 138-142, 2013.

[18] P. K. Balasubramanian, A. Balupuri, and S. J. Cho, "3D QSAR study on pyrrolopyrimidines-based derivatives as LIM2 kinase inhibitors", J. Chosun Natural Sci., Vol. 8, pp. 285-292, 2015.

[19] S. J. Cho, "The importance of halogen bonding: A tutorial", J. Chosun Natural Sci., Vol. 5, pp. 195-197, 2012.

[20] SYBYLx2.1, Tripos International, 1699 South Hanley Road, St. Louis, Missouri, 63144, USA.

[21] R. D. Cramer, D. E. Patterson, and J. D. Bunce, "Comparative molecular field analysis (CoMFA). 1. Effect of shape on binding of steroids to carrier proteins", J. Am. Chem. Soc., Vol. 110, pp. 5959-5967,1988.